First-principles Study of Electronic Structure, Mechanical and Superconducting Properties of Palladium Hydride

S. Kanagaprabha[1*] and R. Rajeswarapalanichamy[2]

[1]*Department of Physics, Kamaraj College, Thoothukudi, Tamilnadu-628003, India.*
[2]*Department of Physics, Nadar Mahajana Sangam S. Vellaichamy Nadar College
(N.M.S.S.V.N College), Madurai, Tamilnadu-625019, India.*

Authors' contributions

*This work was carried out in collaboration between both authors. Author SK designed the study,
performed the statistical analysis, wrote the protocol and wrote the first draft of the manuscript. Author
RR managed the analyses of the study and the literature searches. Both authors read and approved
the final manuscript.*

Article Information

Original Research Article

ABSTRACT

The Structural, electronic and elastic properties of mono and dihydrides of Palladium were
investigated by using first-principles calculation based on density functional theory as implemented
in the Vienna ab-initio simulation package. It was revealed that the calculated lattice parameters
were in agreement with the experimental results. A pressure-induced structural phase transition
from ZB to NaCl was observed at a pressure of 11 GPa for PdH. A high superconducting transition
temperature (T_c) of 18.76 K was obtained for PdH_2.

Corresponding author: Email: skprabha29@gmail.com;

1. INTRODUCTION

Palladium has been known as an excellent metallic observer of hydrogen for more than a century [1]. Electronic structure of $PdH_{0.6}$ at 100K was studied through photoelectron spectroscopy [2]. Skoskiewicz observed superconductivity in the PdH_x system for $x \geq 0.8$ [3]. PdH_x is a superconductor with a transition temperature T_c of about 9 K for x=1 [4]. Band structure calculations and superconducting properties of PdH_x and PdD_x have been reported [5]. Recently, both static and dynamic calculations of various properties of PdH(D) have been performed [6]. Stoichiometric PdH and PdD in a diamond anvil cell have been synthesised and pressure dependence of the superconducting transition temperature was measured [7]. To the best of our knowledge, the structural properties of palladium hydrides have not been reported till date.

In this paper, structural, mechanical and electronic properties of mono and dihydrides of Palladium metal were investigated by the first principles calculation using the Vienna ab-initio simulation package (VASP).

2. COMPUTATIONAL DETAILS

The total energy calculations were carried out using density functional theory (DFT) as implemented in the Vienna ab-initio simulation package (VASP) [8], which is based on pseudo potentials and plane wave basis functions. All electron projected augmented wave (PAW) method of Blochl [9] was applied in VASP with the frozen core approximation. The generalised gradient approximation (GGA) introduced by Perdew, Burke and Ernz-erhof (PBE) [10] was employed to evaluate the electron exchange and correlation potential. The valence electron configurations are Pd $4d^{10}$ and H $1s^1$. The cutoff energy for plane waves in the present calculation was 500 eV. The integration over the Birllouin Zone (BZ) was performed with a grid of special k point-mesh determined according to the Monkhorst-Pack scheme [11] with a grid size of 8x8x8 for structural optimisation and total energy calculation. Iterative relaxation of atomic positions was stopped when the change in total energy between successive steps was less than 1 meV/cell. Pressure calculations were done with second-order Birch Murnaghan equation of states [12,13]. The superconducting transition temperature was obtained using the tight binding

linear muffin tin orbital method (TB-LMTO) within the framework of local density approximation (LDA) [14-17].

3. RESULTS AND DISCUSSION

3.1 Geometric Properties

At ambient condition, the monohydride of palladium crystallise in ZB structure with the space group of *F-43m* (no.216). The wyckoff positions for Pd atom is 4a:(0,0,0) and H atom is 4c:(0.25,0.25,0.25) and contains four formula units per unit cell. The dihydrides of Pd crystallise in CaF_2 structure with the space group of *Fm-3m* (no.225). The cubic unit cell is composed of four formula units with the metal and H atoms in 4a: (0,0,0) and 8c:(0.25,0.25,0.25) sites, respectively. Here, each metal atom is surrounded by eight H atoms forming a cube and each H connects with four metal atoms to build a tetrahedron. The unit cell structures of the considered phases of mono and dihydrides of Pd atoms are given in Fig. 1 (a&b).

3.2 Ground State Properties

The stability of mono and dihydrides of Pd were analysed by computing the formation energy using the following relations:

$$\Delta H_1 = E_{tot}(TMH) - E_{tot}(TM) - (1/2)E_{tot}(H_2)$$
(1)

$$\Delta H_2 = E_{tot}(TMH_2) - E_{tot}(TM) - E_{tot}(H_2)$$
(2)

Where, $E_{tot}(TMH_2)$ and $E_{tot}(TMH)$ are the energies of primitive cells of PdH_2 and PdH, respectively. $E_{tot}(TM)$ and $E_{tot}(H_2)$ are the energies of a transition metal atom and a hydrogen molecule. The energy of the metal and metal hydride is calculated using VASP code, performed in the frame work of density functional theory using the generalised gradient approximation (GGA). The value of heat of formation ΔH for mono and dihydrides are calculated using Equation 1 and Equation 2, respectively. Valence electron density (VED) is defined as the total number of valence electrons divided by volume per unit cell. The computed lattice parameters a and c (Å), equilibrium volume V_0 (Å^3), valance electron density ρ (electrons/ Å^3) and cohesive energy E_{coh}(eV) for mono and
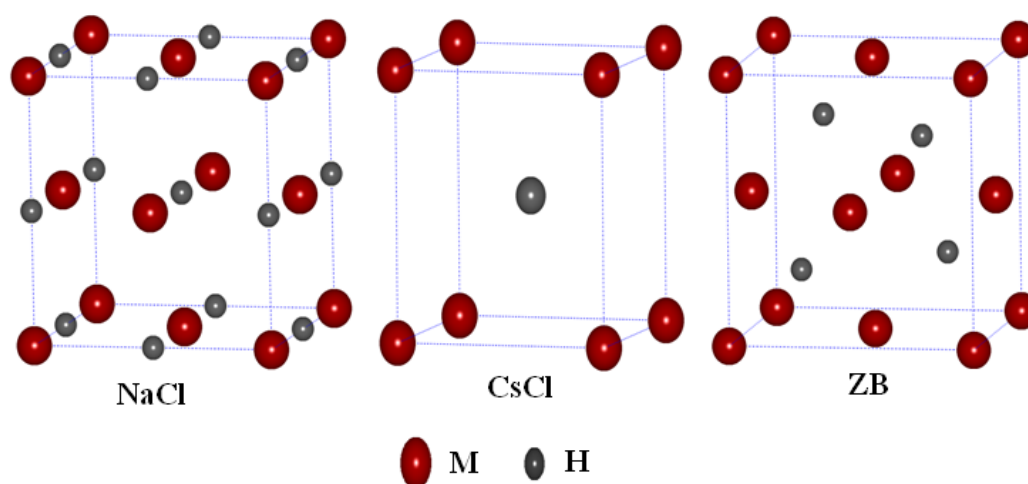
M **H**

Fig. 1a. The unit cell structures of the considered phases of Pdh
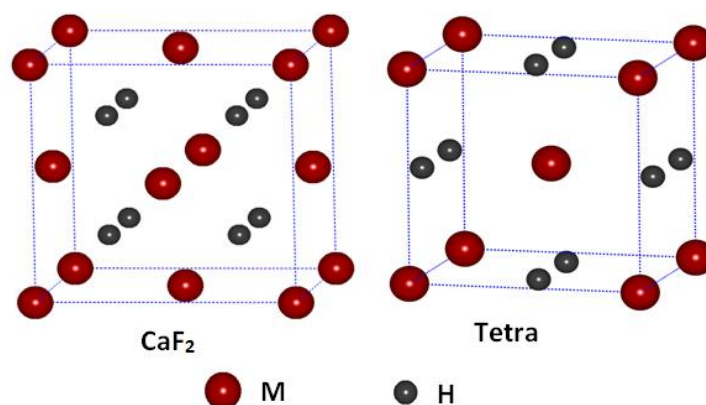

M **H**

Fig. 1b. The unit cell structures of the considered phases of PdH_2

dihydrides of Pd metal for different structures are displayed in Table 1 along with the available data [18,19].

3.3 Structural Phase Transition

The total energy for the considered phases of mono and dihydrides of Pd was calculated as a function of the reduced volume and their plots are given in Fig. 2. It is noted that PdH and PdH_2 were stable in ZB and CaF_2 phases, respectively. On further reducing the volume, a structural phase transition occurred from ZB to NaCl phase in PdH whereas PdH_2 was found to be highly stable in the cubic (CaF_2) phase at ambient and as well at high pressures.

Table 1. Lattice parameters a and c (Å), EquilibriumV_0 (Å^3), Valence electron density (electrons/ Å^3) and cohesive energy E_c (eV)

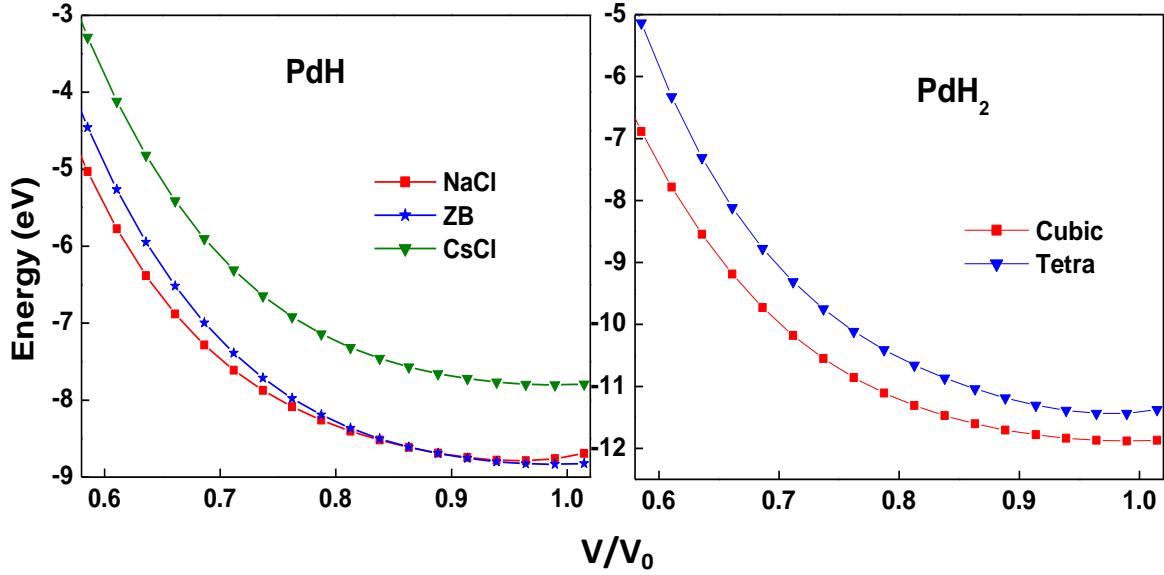|	PdH			PdH_2	
	NaCl	**ZB**	**CsCl**	**Cubic**	**Tetra**
a	4.1440 4.07[18] 4.147[19]	4.2505	2.6746	4.475	3.7912
c	-	-	-	-	3.3552
V_0	17.820	19.240	19.130	22.40	23.46
ρ	0.6173	0.5717	0.5750	0.5357	0.5115
E_c	-4.048 -3.261[19]	-5.692	-4.02711	-4.6563	-4.0943

Fig. 2. The total energy as a function of reduced volume for PdH and PdH$_2$
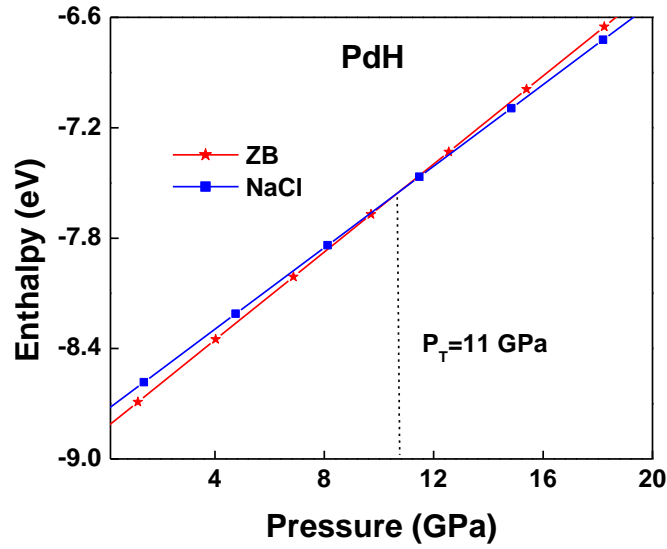

Fig. 3. The enthalpy as a function of pressure of PdH

Table 2. Strain combinations in the strain tensor for calculating the elastic constants of cubic structures

Cubic crystals		
Strain	**Parameters (unlisted e_i=0)**	**$\Delta E/V_0$**
1	$e_1=e_2=\delta$, $e_3=(1+\delta)^{-2}-1$	$3(C_{11}-C_{12})\delta^2$
2	$e_1=e_2=e_3=\delta$	$(3/2)(C_{11}+2C_{12})\delta^2$
3	$e_6=\delta$, $e_3=\delta^2(4-\delta^2)^{-1}$	$(1/2)C_{44}\delta^2$

In order to determine the structural phase transition, enthalpy is calculated using the formula:

$$H=E+PV \qquad (3)$$

and their plot are given in Fig. 3. A pressure-induced structural phase transition from ZB phase to NaCl phase was predicted at a pressure of 11GPa for PdH.

3.4 Elastic Properties

In order to calculate the elastic constants of a structure, a small strain is applied to the structure and its stress is determined. The energy of a strained system [20,21] can be expressed in terms of the elastic constants C_{ij} as:

$$\Delta E = \frac{E(\{e_i\}) - E_0}{V_0} = \left(1 - \frac{V}{V_0}\right) P(V_0) + \frac{1}{2}\left(\sum_1^6 \sum_1^6 C_{ij} e_i e_j\right) + O(\{e_i^3\})$$

(4)

Where, V_0 is the volume of the unstrained lattice, E_0 is the total minimum energy at this unstrained volume of the crystal, $P(V_0)$ is the pressure of the unstrained lattice, and V is the new volume of the lattice due to strain tensor [21]. The elasticity tensor has three independent components (C_{11}, C_{12}, C_{44}) for cubic crystals. A proper choice of the set of strains $\{e_i, i=1,2,.......,6\}$, in Equation (4) leads to a parabolic relationship between $\Delta E/V_0$ ($\Delta E \equiv E-E_0$) and the chosen strain. Such choices for the set $\{e_i\}$ and the corresponding form for ΔE are shown in Table 2 for cubic [22]. For the stable structure of mono and dihydrides of Ni and Pd at normal pressure, the lattice was strained by 0%, ±1%, and ±2% to obtain their total minimum energies E (V). These energies and strains were fitted with the corresponding parabolic equations of $\Delta E/V_0$ to yield the required second-order elastic constants (Table 2).

While computing these energies, all atoms are allowed to relax with the cell shape and volume fixed by choice of strains $\{e_i\}$. From the calculated C_{ij} values, the bulk modulus and shear modulus for the cubic crystals and hexagonal crystals are determined using the Voigt-Reuss-Hill (VRH) averaging scheme [23-25]. The strain energy $1/2C_{ij}e_ie_j$ of a given crystal in Equation (3) must always be positive for all possible values of the set $\{e_i\}$; for the crystal to be mechanically stable. The calculated elastic constants C_{ij}(GPa),Young's modulus E(GPa), shear modulus G(GPa) and Poisson's ratio (v) are listed in Table 3. From tabulated values, it is clear that most of the calculated elastic constants are in agreement with the available theoretical and experimental data [19,26]. The small deviation in some elastic constants may be due to the small difference in the lattice constants calculated by different methods and also upon the various software packages used.

Table 3. Elastic moduli and elastic constants in GPa

	Pd	PdH	PdH$_2$
C_{11}	358.34	184.96 241.7[19]	197.67
C_{12}	206.70	130.2 190.3[19]	131.88
C_{44}	108.37	48.53 69.05[26] 25.5[19]	31.21
B	257.25	148.64 183.32[26]	153.81
G	95.35	40.01	31.88
E	254.59	110.16	89.47
v	0.335	0.38	0.40

The Born-Huang elastic stability criteria [27] for the cubic crystals are

$$C_{44} > 0, \quad C_{11} > |C_{12}|, \quad C_{11} + 2C_{12} > 0$$

(5)

The computed values of the elastic constants for the rare earth metal hydrides satisfy Born-Huang criteria suggesting that all are mechanically stable. The Young's modulus (E) and the Poisson's ratio (v) values are two important factors, necessary to find out the technological and engineering applications of a material. The Young's modulus (E) is given by

$$E = \frac{9BG}{(3B + G)}$$

(6)

Poisson's ratio is associated with the volume change during uniaxial deformation, which is expressed as follows

$$v = \frac{C_{12}}{C_{11} + C_{12}}$$

(7)

The Debye temperature (θ_D) is the important parameter for determining the thermal characteristics of materials, which correlates many physical properties of materials, such as specific heat, elastic constants and melting temperature. The Debye temperature is defined in terms of the mean sound velocity v_m and gives explicit information about the lattice vibrations [28] and it is calculated using the following equation [29].

$$\theta_D = \frac{\hbar}{k_B}\left[6\pi^2 n \frac{N_A \rho}{M}\right]^{1/3} v_m \tag{8}$$

with $\hbar = h/2\pi$, h is Planck's constant, k_B is Boltzmann's constant, N_A is the Avogadro's number, ρ is density, M is molecular weight, n is the number of atoms in the molecule and

$$v_m = \left[\frac{1}{3}\left(\frac{2}{v_t^3} + \frac{1}{v_l^3}\right)\right]^{-1/3} \tag{9}$$

Where

$$v_l = \left(\frac{B + 0.75G}{\rho}\right)^{1/2} \tag{10}$$

And

$$v_t = \left(\frac{G}{\rho}\right)^{1/2} \tag{11}$$

are the velocities of longitudinal and transverse sound waves respectively. The calculated values are listed in Table 4.

Table 4. Density ρ (g/cm^3), longitudinal velocity v_l (km/s), transverse velocity v_t (km/s), average velocity v_m (km/s) and Debye temperature θ_D (K) for mono and dihydrides of Pd

	Pd	PdH	PdH$_2$
ρ	12.007	9.267	8.034
v_l	5.644	4.645	4.943
v_t	2.797	2.038	1.992
v_m	3.139	2.301	2.256
θ_D	381.59	322.25	343.74

3.5 Electronic Structure

In order to understand the electronic structure, total density of states (DOS) for the transition metal (Pd) and for the stable structure of mono and dihydrides of Pd are presented in Fig. 4. The Fermi level is indicated by a dotted vertical line. In the mono-hydrides, the hydrogen character is isolated within the lowest peak, which is a single occupied band holding two electrons. This lowest band possesses significant hydrogen character, in addition to a characteristic free electron tail and some metal character. Along the series, the number of electrons in the d-state increased steadily with the increase in the atomic number. These results indicate a strong hybridisation between the H-1s and M-d states. The central part of the DOS is characterised by two regions. The lower region arises from the hybridisation of p and d states of the transition metal, and the upper region is highly dominated by 4d states. The valence states are separated by a wide gap from the occupied states, indicating covalent behavior. Above the Fermi level, the empty conduction states are present with a mixed s, p, and d characters. Therefore at ambient pressure all these three hydrides showed metallic behavior. The Fermi level is shifted by adding hydrogen.

3.6 Charge Density Analysis

The charge density distribution for PdH and PdH$_2$ containing M$^+$ and H$^-$ ion is shown in Fig.5. It was observed that the voids (i.e., charge depletion regions) are narrow between H ions and broad between the metal ions. On increasing the M-ion atomic number, the M-H bonding becomes stronger and these voids change their shape. It is also found that the light colored areas indicate electron gain, whereas the darker areas indicate electron loss. Because the electron gain on hydrogen is so much greater than on the transition metal, the minimum and maximum values of electron gain and loss were truncated, to keep enough resolution around the transition metals. Electron gain on the hydrogen position is substantial, indicating that the hydrogen does not insert as a bare proton. Near the transition metal there are both regions of positive and negative charge difference, corresponding to the loss or gain of *d* occupation. Significant loss off d state electrons is observed, which may be due to the formation of a bonding-antibonding pair between the direct overlapping of hydrogen *s* with metal *d* orbitals. A more detailed understanding of *d* orbital's gain occupation can be obtained from the total density of states. It is clearly seen that charge strongly accumulates between Pd and H atoms, which means that a strong directional bonding exists between them. It can also be seen that the charge around the Pd site is very much d-like, while that around H site is s-like.

3.7 Superconducting Transition Temperature (T_c K)

One of the important applications of the electronic structure calculations is the determination of the electron-phonon coupling constant, which in turn can be used to estimate the superconducting transition temperature T_c. The superconducting transition temperature is estimated by using the McMillan equation modified by Allen and Dynes [30],

$$T_c = \frac{\omega_{\log}}{1.2}\exp\left[\frac{-1.04(1+\lambda)}{\lambda - \mu^*(1+0.62\lambda)}\right] \tag{12}$$
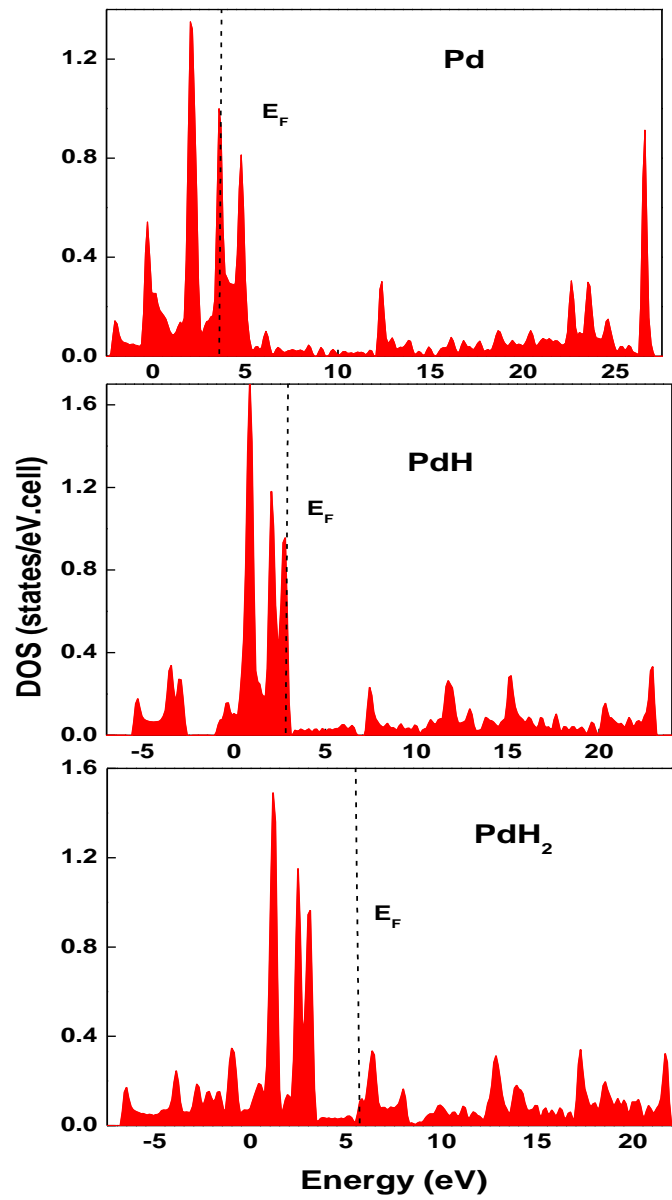
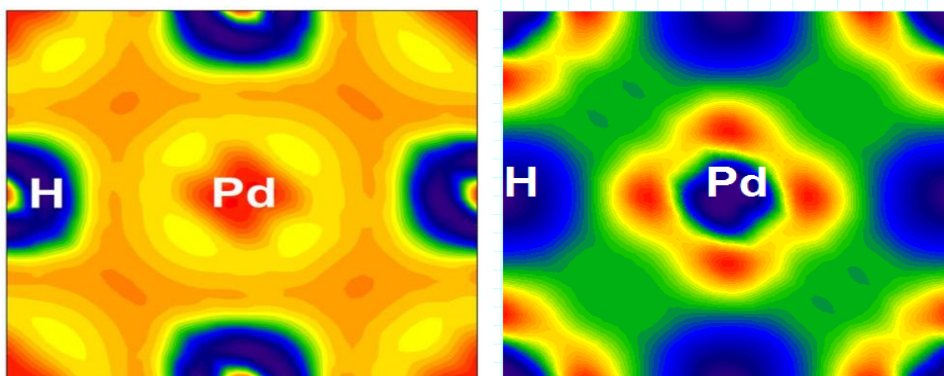**Fig. 4. Density of States of Pd metal, mono and dihydrides of Pd at normal pressure**

Fig. 5. Charge density distribution of mono and dihydrides of Pd

Table 5. λ, μ* and T$_c$ values for mono and dihydrides of Pd

	PdH			PdH$_2$		
	λ	μ*	T$_c$(K)	λ	μ*	T$_c$(K)
Present Expt.	0.378	0.083	8.86 8.0[34] 9.1[35]	1.007	0.047	18.78
Others	0.54[5]	0.085[5]	7.9[5]			

Where, λ is the electron- phonon coupling constant, μ* is the electron - electron interaction parameter and ω$_{log}$ is the average phonon frequency. The average of the phonon frequency square is,

$$<\omega \log^2> = 0.5\,\theta_D^2 \tag{13}$$

The variation of θ$_D$ with pressure in terms of 'E$_F$' and the lattice constant 'a' is given as,

$$\theta_D(P) = \frac{\sqrt{E_F}}{\sqrt{E_F^o}}\frac{a_o}{a}\theta_D \tag{14}$$

But, in this case θ$_D$ is taken as constant for various pressures. θ_D^o, a^o and E_F^o are Debye temperature, lattice constant and Fermi energy corresponding to normal pressure. The electron-phonon coupling constant λ can be written as follows [31].

$$\lambda = \frac{N(E_F)<I^2>}{M<\omega^2>} \tag{15}$$

Where, N (E$_F$) is the density of states at the Fermi energy. M is the atomic mass.

<I^2> is the square of the electron - phonon matrix element averaged over the Fermi energy. <I^2> (in Rydbergs) can be written as [32],

$$<I^2> = 2\sum_l \left\{\frac{(l+1)}{(2l+1)(2l+3)}\right\}M^2_{l,l+1}\left\{\frac{N_l(E_F)N_{l+1}(E_F)}{N(E_F)^2}\right\} \tag{16}$$

Where, M$_{l, l+1}$ are the electron-phonon matrix elements which can be expressed in terms of the logarithmic derivatives.

$$D_l = \frac{d\ln\phi_l}{d\ln r}\bigg|_{r=s} \tag{17}$$

is evaluated at the sphere boundary,

$$M_{l,l+1} = -\phi_l\phi_{l+1}\left[(D_l(E_F)-1)(D_{l+1}(E_F)+l+2)+(E_F-V(S))S^2\right] \tag{18}$$

Where, Φ$_l$ is the radial wave function at the muffin-tin sphere radius corresponding to the Fermi energy. The logarithmic derivative of the radial wave function at the sphere boundary (D$_l$), the muffin-tin potential at the sphere boundary (V(S)) and the radius of the muffin-tin sphere (S) are taken from the output of TB-LMTO program.

The electron – electron interaction parameter μ* is estimated using the relation [33],

$$\mu^* = \frac{0.26N(E_F)}{(1+N(E_F))} \tag{19}$$

The calculated λ, μ*and T$_c$ values for PdH and PdH$_2$ at normal pressure is shown in Table 5. The estimated super-conducting Transition Temperature (T$_c$) was 8.86 K for PdH. It was compared with the available experimental and theoretical work [34,35,5].

4. CONCLUSION

The structural, electronic and elastic properties of mono and dihydrides of Pd have been investigated in detail based on the first-principles calculation. The calculated ground state properties are in good agreement with the other available data. Results from the present study suggest that PdH is stable in ZB phase and PdH$_2$ is highly stable in the CaF$_2$ phase at normal pressure. A pressure-induced structural phase transition from ZB phase to NaCl phase for PdH is predicted at a pressure of 11GPa. The calculated superconducting Transition Temperature of PdH and PdH$_2$ is 8.86K and 18.76 at normal pressure.

ACKNOWLEDGEMENT

COMPETING INTERESTS

Authors have declared that no competing interests exist.

REFERENCES

1. Graham T. On the absorption and dialytic separation of Gases by colloid Septa, Philo. Trans. R. Soc. London. 1866;156: 339-439.
2. Schlapbach L, Burger JP. A new XPS UPS study of the electronicstructure of PdH0.6. J. Physique-Lettres. 1982;43:237.
3. Skoskiewicz T. Superconductivity in the palladium-hydrogen and palladium-nickel-hydrogen systems, phys. Status Solidi (a) 1972;11:K123.
4. Tripodi Paolo, Di Gioacchino Daniele, Vinko Jenny Darja. A review of high temperature superconducting property of pdh system. International Journal of Modern Physics B. 2007;21:3343–3347.
5. Papaconstantopoulos DA, et al. Band structure and superconductivity of PdDx and PdHx, Phys. Rev. B. 1978; 17:141.
6. Shabaev A, Papaconstantopoulos DA. Et al. First-principles calculations and tight-binding molecular dynamics simulations of the palladium-hydrogen system. Phys. Rev. B. 2010;81:184103.
7. Hemmes H, et al, Isotope effects and pressure dependence of the T_c of superconducting stoichiometric PdH and PdD synthesized and measured in a diamond anvil cell. Phys. Rev. B. 1989; 39:4110.
8. Kresse G, Furthm̈uller J. Efficient iterative schemes for ab initio total-energy calculations using a plane-wave basis set, Phys. Rev. B. 1996;54:11169.
9. Blochl PE. Projector augmented-wave method, Phys. Rev. B. 1994;50:17953.
10. Perdew JP, Burke K, Ernzerhof M. Generalized gradient approximation made simple. Phys. Rev. Lett. 1996;77: 3865.
11. Monkhorst HJ, Pack JD, Special points for Brillouin-zone integrations, Phys. Rev. B. 1976;13:5188.
12. Murnaghan FD. The Compressibility of Media under Extreme Pressures, in Proceedings of the National Academy of Sciences. 1944;30:244-247.
13. Francis Birch, Finite Elastic Strain of Cubic Crystals, in Physical Review. 1947;71:809-824.
14. Skriver HL. The LMTO method. Springer, Heidelberg; 1984.
15. Anderson OK. Linear methods in band theory, Phys. Rev. B. 1975;12:3060.
16. Anderson OK, Jepson O. Explicit, first-principles tight-binding theory. Phys. Rev. lett. 1984;53:2571.
17. Anderson OK, Jepson O, Sob M. Electronic band structure and its applications, Editors. M. Yussouff. Springer Verlag Lecture Notes; 1987.
18. Fukai Y, Okuma N. Formation of superabundant vacancies in pd hydride under high hydrogen pressures. Phys. Rev. Lett. 1994;73:1640.
19. X.Zhou et.al, An embedded-atom method interatomic potential for Pd–H alloys, J. Matt. Res. 2008;23:704-718.
20. Nye JF. Physical Properties of Crystals, Oxford; 1985.
21. Wu SQ, Hou ZF, Zhu ZZ. Ab initio study on the structural and elastic properties of MAlSi (M=Ca, Sr, and Ba), Solid State Comm. 2007;143:425-428.
22. Kalay M, Kart HH, Çagin T. Elastic properties and pressure induced transitions of Zno polymorphs from first-principle calculations. J. Alloys Compd. 2009;484:431-438.
23. Voigt W. Lehrbuch de Kristall physik (Terubner, Leipzig); 1928.
24. Reuss A, Angew Z. Berechnung der Fließgrenze von Mischkristallen auf Grund der Plastizitätsbedingung für Einkristalle, Math. Mech. 1929;9:49-58.
25. Hill R. The elastic behavior of a crystalline aggregate, Proc. Phys. Soc., London, Sec. A. 1952;65:349.
26. Hsu DK, Leisure RG. Elastic constants of palladium and β-phase palladium hydride between 4 and 300 K, Phy. Rev. B. 1979; 20:1339.
27. Born M, Huang K. Dynamical Theory of Crystal Lattices, Clarendon, Oxford; 1956.
28. Ibrahim AM. Ion beam mixing of metals and Debye temperature, Nucl. Instrum. Meth. B. 1988;34:135.
29. Anderson OL. A simplified method for calculating the debye temperature from elastic constants. J. Phys. Chem. Solids. 1963;24:909-917.
30. Allen PB, Dynes RC. Transition temperature of strong-coupled super-

conductors reanalyzed. Phys. Rev. B. 1975;12:905.

31. McMillan WL. Transition temperature of strong-coupled superconductors. Phys. Rev. B. 1968;167:331.

32. Skriver HL. Mertig I. Crystal structure from one-electron theory. Phys. Rev. B. 1985; 32:4431.

33. Bennemann KH, Garland JK. Super-conductivity in d and f-band metals, in:

Douglass DH. (Ed.). American Institute of Physics, Newyork; 1971.

34. Schirber JE, Northrup CJM. Concentration dependence of the superconducting transition temperature in PdHx and PdDx. Phy. Rev. B. 1974;10:3818-3820.

35. Miller RJ, Satterthwaite CB. Electronic model for the reverse isotope effect in superconducting Pd-H(D). Phy. Rev. Letter. 1975;34:144.

Peer-review history:
The peer review history for this paper can be accessed here:
http://www.sciencedomain.org/review-history/26021